Asian Journal of Chemistry; Vol. 34, No. 7 (2022), 1755-1762

ASIAN JOURNAL OF CHEMISTRY

https://doi.org/10.14233/ajchem.2022.23787


# Silver Nanoparticles Mediated through Aqueous Leaf Extract of *Ageratina adenophora* Inhibit Proliferation and Induce Apoptosis in Human Ovarian Teratocarcinoma Cell Line PA-1

B. Latha Maheswari*, N. Mani, S. Karthika and N. Kavikala

PG and Research Department of Chemistry, A.V.V.M. Sri Pushpam College (Affiliated to Bharathidasan University), Poondi-613503, India

*Corresponding author: E-mail: rajilatha54@gmail.com

*Received*: 17 February 2022; *Accepted*: 20 March 2022; *Published online*: 15 June 2022; AJC-20851

An enhanced anticancer properties of *Ageratina adenophora* mediated silver nanoparticles (AgNPs) were evaluated in the present study. The biogenic AgNPs effectively inhibited the viability and proliferation of ovarian teratocarcinoma cells (PA-1) by significantly increasing the initiation of apoptosis. The AgNPs were synthesized with the phytochemicals present in aqueous extract of *Ageratina adenophora* leaves which performed the dual function of reducing silver ions as well as the capping the nanoparticles. Characterization of nanoparticles with UV-vis spectroscopy revealed surface plasmon resonance peak at 470 nm. Fourier transform infrared spectrum showed the presence of functional groups such as alcohol, aldehyde, alkane, aromatic amines and phenolic compounds. X-Ray diffraction (XRD) analysis revealed the crystalline nature and face centred cubic structure of AgNPs. The size, morphology and distribution of AgNPs were confirmed with scanning electron microscope (SEM). Further, dynamic light scattering (DLS) and zeta potential measurements also confirmed the size and charge of the synthesized nanoparticles. The AgNPs significantly increased the cytotoxicity and inhibited the proliferation of PA-1 cells. Apoptosis of PA-1 cells were increased with treatment of AgNPs. The increased cytotoxicity of PA-1 cells was due to the synergistic activity of phytochemicals and AgNPs. Hence, the current research on the silver nanoparticles mediated through *A. adenophora* leaf extract could be an effective alternative in treatment of ovarian cancer.

**Keywords: *Ageratina adenophora*, Silver nanoparticles, PA-1 cells, Ovarian cancer, Apoptosis.**

## INTRODUCTION

Cancer is a complex form of macabre illness which is characterized by uncontrolled multiplication of cells resulting in abnormal growth and accumulation and causes tissue damage [1]. Among the different types of cancer, ovarian cancer is the seventh leading cause of infirmity and fatality [2]. It is a complex neoplastic assembly that affects women above the age group of 65 [3]. The heterogeneous population of ovarian cancer cells exhibit high level of tumourigenicity and differentiation. Globally, 4.4% of ovarian cancer incidence, accounting to 1,84,799 cases were reported during 2018 [4] and it is estimated that the disease incidence might raise to 55% by 2035 [5]. India ranks first among Asian countries with high rate of mortality [6]. The challenge in the ovarian cancer treatment is its multiple histo phenotypes and sites of origin [7]. Hence, the therapeutic efficiency of a potent ovarian cancer drug depends on the potential to distinguish and target specific cancer cells [8]. The conventional therapy in the treatment of cancer includes chemotherapy, hormonal therapy, neo-adjuvant therapy, immune therapy, gene therapy, surgery and targeted therapy. Besides, multiple therapeutic options, still high rate of relapse is reported due to delayed identification, difficulty in early diagnosis and exorbitant cost involved in treatment. Further, currently employed chemotherapeutic agents are not tissue specific and accompanied with adverse effects. Hence, the current research interest is directed towards the exploration of simple and green treatment procedures for cancer that utilizes natural products with unchallenged therapeutic potential [1,9,10].

Medicinal plants are potential resource of bioactive compounds for the development of drugs [11]. WHO states that globally 80% of people from under developed and developing countries still rely on the practice of traditional medicine for their primary healthcare needs. The demand and acceptance of medicinal plants in traditional medicinal system is due to

its easy availability, cost effectiveness and the minimal side effects exerted by the phytochemicals [12]. The phytochemicals exhibit effective chemopreventive properties and hence considered as important fount of natural anticancer drugs. *Ageratina adenophora* is a perennial herb native to Mexico and widely distributed in America, Africa, China and throughout the Indian subcontinent. The plant belong to Asteraceae family and contains various secondary metabolites and bioactive phytochemicals including essential oils, phenyl propanoids, terpenoids, tannins, glycosides, flavonoids, sterols, alkaloids, coumarines, *etc.* [13-16]. *Ageratina adenophora* was reported to possess antibacterial, antifungal [17], larvicidal [18], anti-inflammatory [19], antipyretic [20], antioxidant [21], analgesic [22], antitumour [23], insecticidal [24] and antiviral activities [25]. Mani *et al.* [26] reported the phytochemicals present in leaves of *Ageratina adenophora* are potent alternative medication for the treatment of lung cancer.

Nanomaterials differ from their bulk counterparts and exhibit unique competencies in terms of its low volume to surface area, physico-chemical and thermodynamic properties [27,28]. Though the physical and chemical method for the synthesis of nanoparticles is simple, they require intensive energy and utilize toxic chemicals for reduction of metal ions as well as stabilizing the biogenic silver nanoparticles. In particular, the capping agents such as poly(ethylene glycol), poly(vinyl alcohol) and poly(vinyl pyrrolidone) are highly toxic and non-biodegradable [29]. But the biogenic synthesis of nanoparticles based on green chemistry approach is environmentally compatible [30-32] in which the phytochemicals present in plant extract act as reducing and stabilizing agents. Further, the ease in the large scale synthesis of refined and elegant nanoparticles with well-defined size and morphology makes the green chemistry approach as an effective alternative [33]. Previous literatures have reported that the plant extract mediated nanoparticles exhibit enhanced anticancer properties [34,35]. The conjugation of plant derived bioactive compounds with nanoparticles boosts their molecular properties and efficiency to provide improved therapeutic activity. Among the various metallic nanoparticles, silver nanoparticles are reported to possess effective anticancer activity and are potential cytotoxic agents [36,37]. The AgNPs exhibit cytotoxicity in cancer cells by inducing apoptosis through different mechanisms such as mitochondria dependent and independent pathways, leakage of lactate dehydrogenase, generation of reactive oxygen species and by mitochondrial dysfunction [29,38-43]. Besides these molecular mechanisms, the anticancer activity of AgNPs also depends on its structural and morphological characteristics, surface coating of phytochemical, charge and the target cell in which they act. Hence, this study is aimed to evaluate the cytotoxic potential of AgNPs in initiating apoptosis in human ovarian teratocarcinoma cell line PA-1.

## EXPERIMENTAL

Dulbecco's modified Eagle's medium (DMEM), streptomycin, penicillin-G, phosphate buffered saline, 3-(4,5-dimethylthiazol-2-yl)-2,5-diphenyltetrazoliumbromide (MTT), 2′7′-diacetyl dichlorofluorescein, acridine orange, ethidium bromide, rhodamine-123, dimethyl sulfoxide (DMSO) and bovine serum albumin were purchased from Sigma-Aldrich Chemicals Pvt. Ltd. (India). Analytical grade chemicals purchased from Himedia Pvt. Ltd. were used in the study.

**Preparation of aqueous extract:** Fresh healthy leaves of *Ageratina adenophora* collected from Kodaikanal hills, India were used. The leaves were washed with tap water and then with distilled water to remove any surface contaminations. The leaves were then shade dried for 10 days and macerated into a fine powder. Leaf powder (5 g) was dissolved in 100 mL of distilled water and boiled to 70 ºC for 30 min. The leaf extract was cooled at room temperature and filtered using Whatman filter paper no. 1. The filtrate was stored at 4 ºC until further studies.

**Green synthesis of AgNPs:** The prepared leaf extract of *A. adenophora* and 3 mM $AgNO_3$ solution was added in equal proportion at a ratio of 1:1. Plant extract (50 mL) was titrated slowly to 50 mL of aqueous silver nitrate solution. The pH was adjusted to 10 with 1 M NaOH and incubated for 0.5 h at 70 ºC [44]. The change in the colour of the reaction mixture from brown to dark greenish black colour indicate the reduction of $Ag^+$ to $Ag^0$ and the formation of silver nanoparticles.

**Characterization:** The characterization of biosynthesized AgNPs were carried out using UV-vis spectroscopy with the wavelength ranging from 200-800 nm. FTIR analysis was carried out to identify the functional groups, XRD to confirm the synthesis, size and crystallinity, dynamic light scattering analysis (DLS) to determine the size of AgNPs and SEM to identify the morphology of the synthesized AgNPs. The EDAX analysis was carried out to determine the elemental composition of the synthesized nanoparticles. The surface charge of nanoparticles was determined with zeta potential measurements.

**Cell culture maintenance:** PA-1, ovarian carcinoma cell lines were procured from National Centre for Cell Sciences, Pune, India. The cell lines were maintained in Dulbecco's Modified Eagle Media (DMEM) supplemented with 10% Fetal Bovine Serum (FBS). Penicillin (100 U/mL) and streptomycin (100 µg/mL) and maintained in a humidified environment with 5% $CO_2$ at 37 ºC.

**Cell viability (MTT) assay:** Approximately, $1 \times 10^4$ cells/well (200 µL) of PA-1 cells were seeded into 96 well plate. After 24 h of confluence cell growth, 100 µL of various concentrations of AgNPs (5, 10, 15, 20, 25 and 30 µL/mL were added to the culture medium and incubated at 37 ºC for 24 h. Finally, 5 mg/mL of MTT (3-[4,5-dimethyl thiazol-2-yl]-2,5-diphenyltetrazolium bromide) prepared with phosphate buffer was added to each well and incubated for 4 h at 37 ºC. The purple coloured precipitate, formazon was dissolved in 100 µL of DMSO and measured at an absorbance of 540 nm using ELISA plate reader [45]. The experiment was carried out in triplicate and the survival rate was determined using the formula:

$$\text{Cell viability (\%)} = \frac{1 - \text{Absorbance of treated cells}}{\text{Absorbance of control cells}} \times 100$$

**Cell morphology:** The morphological changes of PA-1 cells were examined by plating the cells in 6 well plates ($1 \times 10^5$ cells/wells) and incubated with 20 and 25 µg/mL concentrations of AgNPs. A control was also maintained without the

addition of AgNPs. The cell morphology of both the treated and untreated cells were observed using an optical microscope (OLYMPUS IX71 microscope, Tokyo, Japan) with appropriate filter sets after 24 h of post treatment [46].

**Measurement of reactive oxygen species:** Intracellular ROS level was determined by a previously described method using 2,7-dichloro-dihydrofluorescein diacetate (DCFH-DA) assay [47]. Approximately $2 \times 10^6$ cells/well (PA-1 cells) were seeded in 6 well plate and allowed to attach for 24 h. Incubation was followed by the addition of AgNPs (20 and 25 µg/mL) and further incubated with 5% $CO_2$ at 37 ºC. The overnight grown, PA-1 cells were washed twice with PBS and supplemented with 25 µM DCFH-DA and the incubation was continued at 37 ºC for 30 min. The cells were then rinsed with PBS and each well was added with 2 mL of PBS. The intensity of fluorescence was measured spectroflurometrically for every 5 min for a period of 30 min with excitation at 485 nm and emission at 530 nm.

**Mitochondrial membrane potential:** Mitochondrial membrane potential (MMP) was determined following the method as described by Bhosle *et al.* [48]. PA-1 cells seeded on to 6 well plate with cover slip were treated with different concentrations (20 and 25 µg/mL) of AgNPs. Rh-123 dye was used to stain the PA-1 cells. After the addition of dye the cells were incubated for 30 min and washed with PBS twice and fixed. The intensity of fluorescence was measured at 535 nm. Low fluorescence emission indicate the loss of mitochondrial membrane potential in PA-1 cells.

**Apoptotic induction:** The influence of AgNPs on the initiation of apoptosis in PA-1 cells was examined using fluorescence microscopic analysis following the methodology of Baskic *et al.* [49]. PA-1 cells of concentration of $5 \times 10^4$ cells/well were seeded in a six well plate and incubated for 24 h. and treated with 20 and 25 µg/mL concentration of AgNPs. After the treatment with AgNPs, the cells were incubated for 24 h, detached from the wells and washed with cold PBS thrice. Then the cells were stained using acridine orange/ethidium bromide at 1:1 ratio (100 µg/mL) for 5 min and examined under fluorescent microscope at 40X magnification. The number of cells exhibiting apoptotic features was determined with the emission of orange/yellow fluorescence.

**Colony inhibition assay:** The inhibition of colony formatting ability of PA-1 by biosynthesized AgNPs was evaluated by a previously described protocol of Franken *et al.* [50] with minor modifications. The PA-1 cells were seeded on to a 48 well plate (approximately 100 cells/well) and were allowed to adhere to the surface of the well for 18 h. Then the cells were treated with AgNPs (20 and 25 µg/mL). A control without the treatment of AgNPs was also maintained. Both the treated and untreated (control) cells were incubated at 37 ºC for 14 days. After incubation the cells were visualized under microscope to determine the reduction in number of colonies compared to that of untreated cells.

## RESULTS AND DISCUSSION

The green chemistry mediated AgNPs were prepared using aqueous solution of *A. adenophora* leaf extract and $AgNO_3$. The optimal conditions for synthesis of AgNPs was initially screened at 70 ºC, pH = 8 and the stoichiometric concentration of plant extract and $AgNO_3$ solution (1:1 ratio) was fixed. For the preparation of AgNPs 5% solution of plant extract (50 mL) and 3 mM $AgNO_3$ (50 mL) were added and the pH was adjusted to 10 using NaOH. Dropwise addition of plant extract to silver nitrate solution changed the colour of the solution from light brown to dark greenish black colour. The synthesized nano solution was allowed to stand at room temperature for 18 h under dark conditions for the complete saturation of nanoparticles. The change in the colour of the solution due to surface plasmon resonance of silver ions indicated AgNPs synthesis. The formation of AgNPs was then confirmed with UV-vis spectroscopic study which revealed an absorbance peak at 470 nm (Fig. 1a). The reduction of silver ions might be attributed to the role of phytochemicals (secondary metabolites) present in the leaf extract. Further these bioactive compounds also are involved in surface coating of synthesized nanoparticles which preventing the aggregation of nanoparticles and led to stabilization of nanoparticles. A previous report by Ingarasal *et al.* [51] documented that the silver nanoparticles mediated through aqueous extract of *Woodfordia fruticosa* flower extract exhibited SPR peak at 470 nm.

The interaction of secondary metabolites with biosynthesized nanoparticles was examined with FTIR to find out the possible functional groups of plant bioactive compounds that coated the surface of nanoparticles. The FTIR spectrum (Fig. 1b) showed absorbance peaks at 3937.98 $cm^{-1}$, 3769.14 $cm^{-1}$, 3206.64 $cm^{-1}$ which indicated the presence of OH-stretch of alcohol [52,53]. The CH-alkane and aldehyde stretch was represented by the peak at 2974.18 $cm^{-1}$ [54]. The absorbance peak at 2901.59 $cm^{-1}$ indicated the C-H stretch of methyl group [55]. The C=C aromatic alkane is represented by the peak at 1581.21 $cm^{-1}$ [56]. Similarly, the asymmetric stretch of methyl compound was identified with peak at 1257.67 $cm^{-1}$ [56]. The peaks at 1030.42 $cm^{-1}$ and 799.57 $cm^{-1}$ showed the C-O stretch of alcohol and C=C bend, respectively [55]. Aliphatic bromo and iodo compounds were reported with peaks at 687.94 $cm^{-1}$ and 571.67 $cm^{-1}$ [57]. From the FTIR analysis, it could be concluded that alcohol, aldehyde, alkane, methyl, aromatic amines, bromo and iodo compounds present in alkaloids, phenolic compounds, aminoacids, carbohydrates and tannins were involved in the reduction of silver as well as capping of AgNPs. The XRD analysis revealed the crystal nature and structure of the synthesized AgNPs (Fig. 1c). The crystal plane showed intense peak at 2θ angles of 38.23º, 44.51º, 64.41º and 77.51º corresponding to miller index of 111, 200, 220 and 311 (JCPDS No.: 04-0783). These plane of indices confirmed that the synthesized silver nanoparticles were crystalline in nature and had a face centred cubic structure. Further, the analysis of peaks using Scherrer's equation revealed the average particles size of 84 nm. The XRD pattern obtained in the present study was in agreement with the diffraction pattern of an earlier report obtained with AgNPs mediated through aqueous leaf extract of *Andrographis paniculata* [57]. The surface morphology and shape of the synthesized AgNPs were confirmed with SEM studies. The SEM images showed that the AgNPs

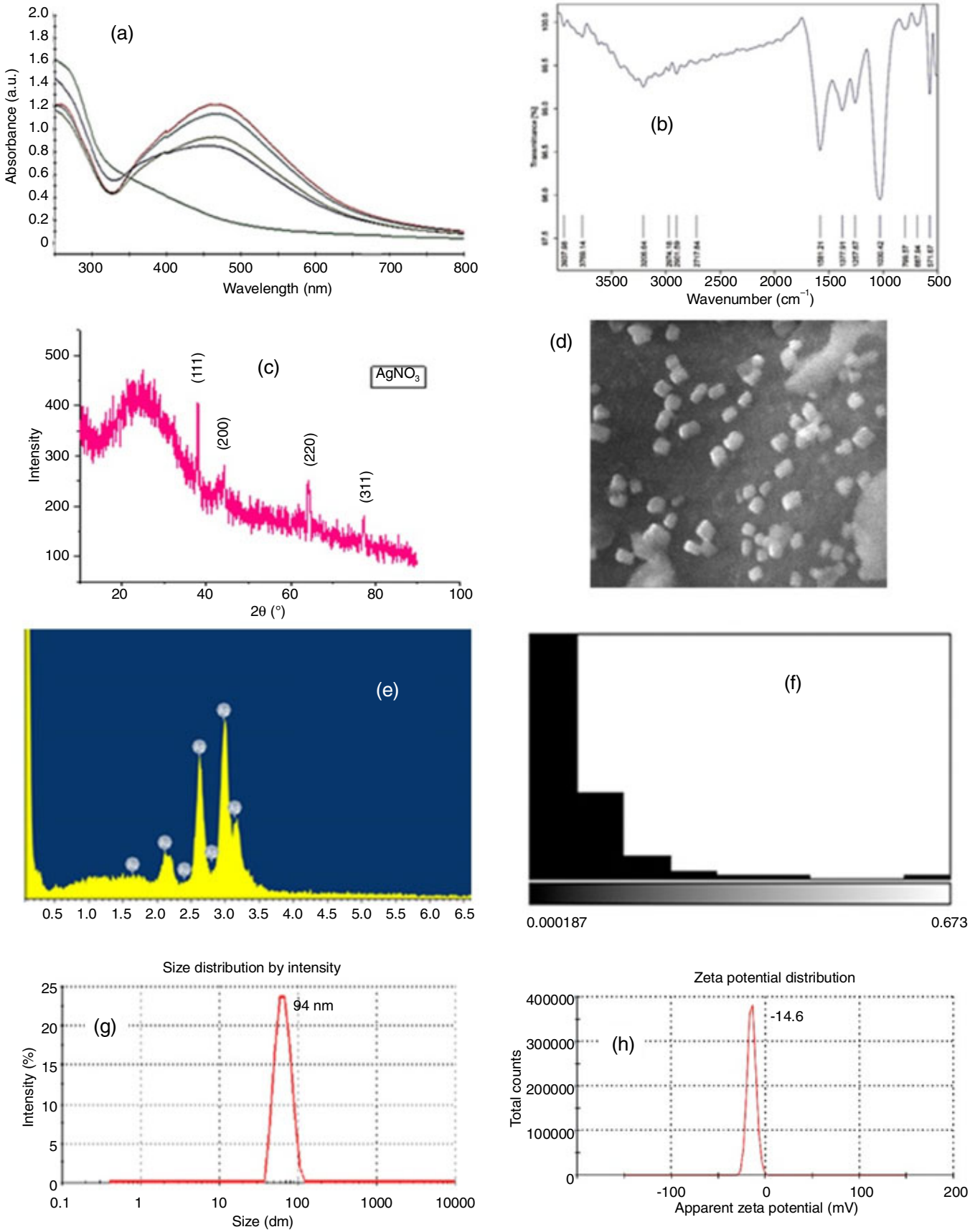


Fig. 1. Characterization of AgNPs (a) UV absorption spectrum showing SPR peak at 470 nm, (b) FTIR spectrum of AgNPs, (c) XRD diffraction spectrum, (d) SEM image of AgNPs, (e) EDAX showing elemental composition, (f) size distribution of AgNPs, (g) DLS indicating the size of AgNPs, (h) zeta potential distribution

were spherical in shape and free from aggregation (Fig. 1d). Further, the EDAX spectrum also showed the presence of silver in high proportion compared to other metals (Fig. 1e). AgNPs with spherical shaped structures were reported with biogenic synthesis using *Butea monosperma* flower extract [58]. The distribution pattern of AgNPs was analyzed to determine the toxicity of nanoparticles, as the smaller sized nanoparticles induce high toxicity due to effective penetration into cell. The DLS analysis indicated that the AgNPs were 94 nm in diameter (Fig. 1g). A slight increase in the particle size compared with that of XRD measurement might be due to presence of water molecules surrounding the nanoparticles. The zeta potential of the nanoparticles confirmed the surface charge to be -14.6 mV (Fig. 1h). This negative charge of the nanoparticles is responsible for their stability and distribution [59].

**MTT assay:** The cytotoxic response of *A. adenophora* mediated AgNPs was evaluated with MTT assay and the outcomes of the study are presented in Fig. 2. The cytotoxicity exerted on PA-1 cells were found to be dose dependent as the viability of PA-1 cells decreased rapidly with increase in concentration of AgNPs. The < 50% cell viability was observed with AgNP concentration above 25 µg/mL. The median inhibitory concentration ($IC_{50}$) of AgNPs was found to be 18.80 µg/mL after 24 h. Mani *et al.* [26] reported the cytotoxic effect of methanolic extract of *A. adenophora* leaves against lung cancer cell (A549) lines with an $IC_{50}$ values of 60.13, 50.8 and 43.28% with 20, 40 and 60 µg/mL. Yuan *et al.* [60] reported that AgNPs are effective in inducing loss of cell viability in ovarian cancer cell lines (A2780) compared to the anticancer agent gemcitabine. The toxicity of AgNPs is regulated by the size of the nanoparticles as smaller particles readily penetrate the cell membrane. Khanra *et al.* [61] reported that synthesized AgNPs from *Asparagus racemous* root extract were effective in inducing loss of cell viability against ovarian cancer cells PA-1. Similarly, the AgNPs mediated through *Boerhavia erecta* leaf extract was also reported to be effective against PA-1 cells [62].

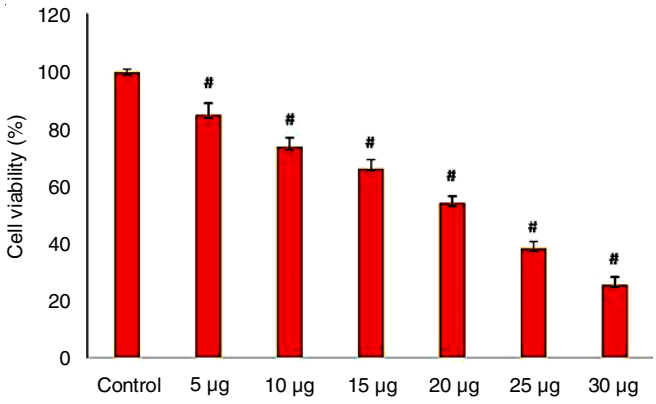


Fig. 2. Dose dependent effect of AgNPs on cell viability of PA-1 cells

**Effect of AgNPs on the morphology of PA-1 cells:** The morphological changes in PA-1 cells due to AgNP treatment with 20 and 25 µg/mL concentration was depicted in Fig. 3. A control (untreated cells) was maintained. Upon visualization after 24 h of post treatment, the control cells were found to proliferate rapidly and reached confluence. But the PA-1 cells treated with AgNPs showed characteristics of apoptotic cell death such as loss of surface adherence, intensive blebbing and cellular fragmentations [63]. Gurunathan *et al.* [64] suggested that AgNPs potentially influence the morphology of ovarian cancer cells. Yuan *et al.* [65] also reported similar morp-hological variations in AgNPs treated ovarian cancer cell lines (A2780). The AgNPs synthesized using *Croton bonplandianum Baill* leaves showed effective morphological alterations in PA-1 cells [66]. Increasing concentration of AgNPs synthesized using *Alpenia purpurata* showed cellular aggregation and formed round structured dead cells [67].

**Effect of AgNPs in the generation of ROS (DCFH-DA staining assay):** ROS has a dual role in both promoting as well as interrupting the process of carcinogenesis [68,69]. ROS produced in minimal quantity helps in normal functioning of a cell, were as high level cause's cellular damage. The production of ROS in the presence of oxygen species is generally catalyzed by silver ions and AgNPs are effective in inducing oxidative stress by increasing the ROS production in human ovarian cancer cells [64] and other cancer cells [60,70,71]. In present study, the ability of AgNPs to generate high intracellular ROS in PA-1 cells was determined with DCFH-DA assay. The results indicate significant dose-dependent activity after 24 h of post-treatment with different concentration of AgNPs (20 and 25 µg/mL). Increase in the level of intracellular ROS in PA-1 cells compared to control cells was clearly visible with increased fluorescence as observed with fluorescence microscope (Fig. 4). Fahrenholtz *et al.* [72] also reported that 10 µg/mL concentration of AgNPs was effective in inducing

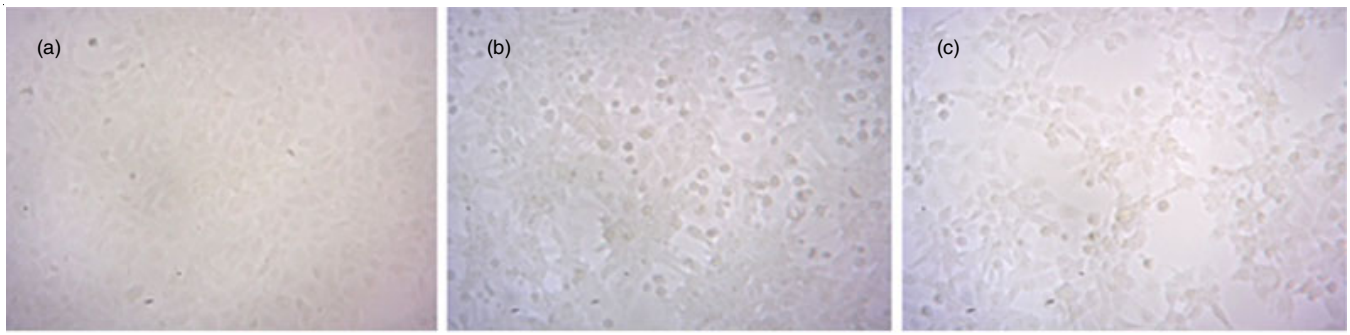


Fig. 3. Morphological changes in PA-1 cells such as shrinkage, detachment, membrane blebbing and distorted shape induced by AgNPs treatment (a) Control (b) 20 µg/mL AgNPs (c) 25 µg/mL AgNPs

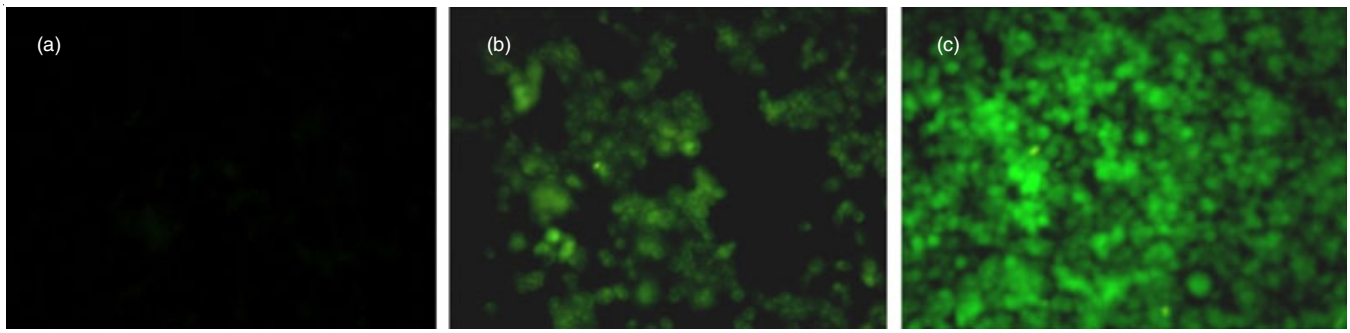


Fig. 4. PA-1 cells treated with AgNPs emitted green fluorescence indicating the generation of ROS (a) Control (b) 20 µg/mL AgNPs (c) 25 µg/mL AgNPs

ROS production in A2780 and SKOV3 cells. But an increase in concentration of AgNPs (> 100 µg/mL) did not showed any significant increase in ROS in A2780 cells.

**Mitochondrial membrane potential (rhodamine 123 dye staining assay):** Mitochondrion plays a vital role in the energy metabolism of all type cells including cancer cells [73]. Cellular metabolism involves the generation of ROS, the most important factor essential for redox signalling. But the abnormal increase in intracellular ROS affects the electrochemical potential of mitochondrial membrane [74] and causes cell death [75]. In present study the early symptom of apoptosis, the loss of MMP, was assessed using rhodomine 123 dye. Fig. 5 represents the effect of AgNPs (20 and 25 µg/mL) on mitochondrial membrane potential in PA-1cells. AgNPs treated PA-1 cells exhibited low emission of fluorescence indicating the loss of membrane potential while the untreated (control) cells had high intensity of green fluorescence as no loss of membrane potential was exerted.

**Apoptotic induction (acridine orange/ethidium bromide staining assay):** Acridine orange/ethidium bromide fluorescent staining is an effective procedure for classifying the normal, apoptotic and necrotic cells. Acridine orange and ethidium bromide are nucleic acid binding dyes, in which acridine orange stains both live and dead cells while ethidium bromide specifically stains injured cells. The live cells produce green fluorescence and the dead cells give orange to yellow fluorescence when stained with this dye. Apoptotic cells produce orange/yellow fluorescence due to DNA fragmentation and chromatin condensation. PA-1 cells treated with AgNPs emit orange to red stain due to induced apoptotic cell death caused by cell membrane disintegration (Fig. 6). Similar fluorescent pattern was observed with ovarian cancer cell line (A2780) treated

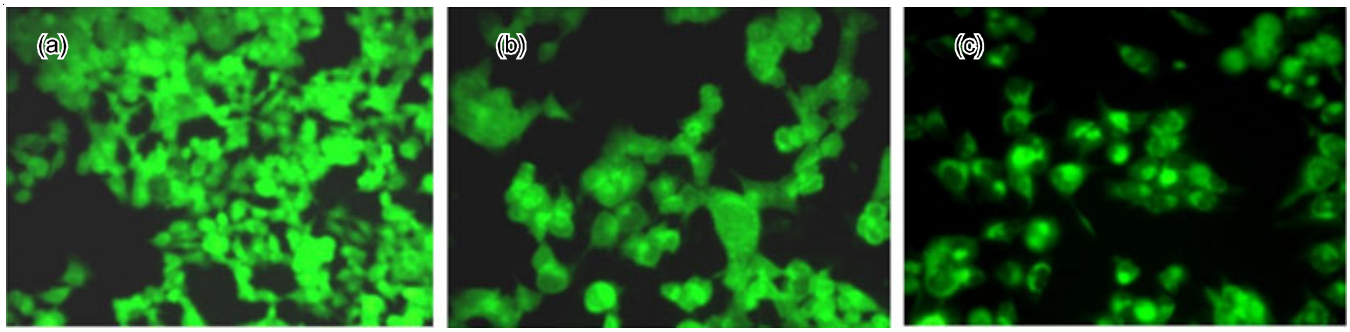


Fig. 5. PA-1 cells treated with AgNPs showed low fluorescence intensity indicating decreased MMP while the control cells showed bright fluorescence due to accumulation of Rh-123 dye (a) Control (b) 20 µg/mL AgNPs (c) 25 µg/mL AgNPs

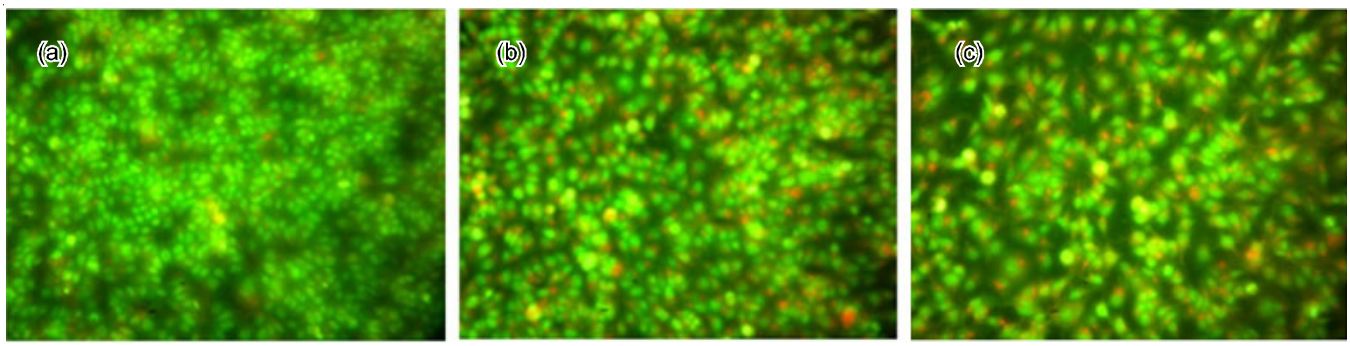


Fig. 6. Dual staining of PA-1 cells with AO/EB showed the nucleus of live cells were stained green, early apoptosis cells exhibited condensed/fragmented nucleus in yellow and late apoptotic cells were found to have condensed/fragmented nucleus with orange fluorescence (a) Control (b) 20 µg/mL AgNPs (c) 25 µg/mL AgNPs

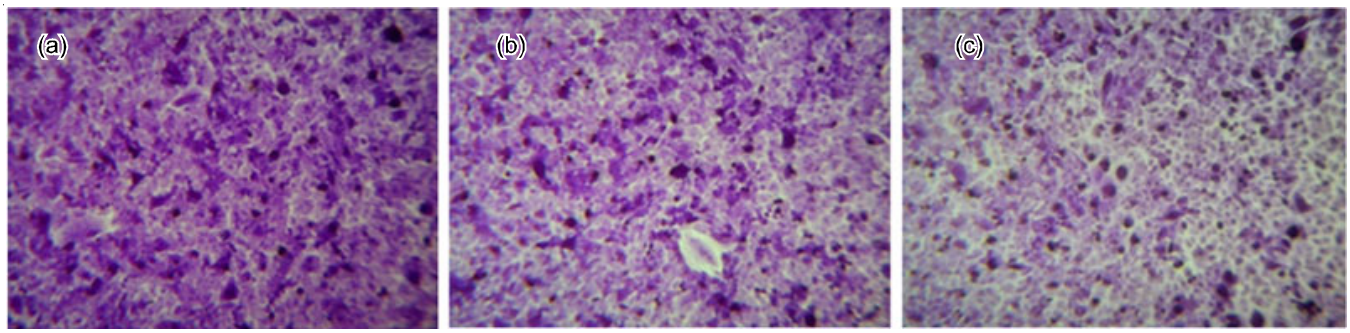


Fig. 7. PA-1 cells treated with AgNPs showed effective reduction in the number of colony formation (a) Control (b) 20 µg/mL AgNPs (c) 25 µg/mL AgNPs

with ruthenium complexed with carbazole based hydrazone [76].

**Colony inhibition:** The capacity of AgNPs to impair the colony forming ability of PA-1 cells were evaluated following the protocol of Franken *et al.* [50] with slight modifications. The PA-1 cells were cultured with the addition of AgNPs for a period of 14 days and assessed for its ability to form colonies. The formations of colonies were observed under microscope after being stained with crystal violet. From the microscopic identification of PA-1 cells, it was evident that AgNPs treated cancer cells showed fewer numbers of colonies compared to untreated cells (Fig. 7). A similar reduction in the number of colonies formed by ovarian cancer cells (A2780) and $ALDH^+$/$CD133^+$ cells with the treatment of AgNPs was reported by Choi *et al.* [77].

## Conclusion

Therapeutic efficacy of commercially available synthetic drugs including chemopreventive agents are accompanied with severe side effects. Also, the cancer treatment is complex and requires personalized or individualistic approach for effective management based on the type of disease. The present work aimed to develop new modality for the treatment of cancer using *in vitro* culture. Thus, the study provides evidences that PA-1 cells were sensitive to AgNPs mediated through *A. adenophora* leaf extract. AgNPs exhibited strong anticancer effects against PA-1 cells by inducing cytotoxicity, morphological and nuclear changes. Further these AgNPs were also found to induce ROS production and decrease mitochondrial membrane potential there by initiating apoptosis in PA-1 cells. The study also recommends further research to define different subsets of ovarian cancer cells that are susceptible to treatment with AgNPs mediated through green chemistry concept.

## CONFLICT OF INTEREST

The authors declare that there is no conflict of interests regarding the publication of this article.

## REFERENCES

1. M.E.A. El-Hack, S. Abdelnour, M. Alagawany, M. Abdo, M.A. Sakr, A.F. Khafaga, S.A. Mahgoub, S.S. Elnesr and M.G. Gebriel, *Biomed. Pharmacother.*, **111**, 42 (2019); https://doi.org/10.1016/j.biopha.2018.12.069
2. S.H. Hassanpour and M. Dehghani, *J. Cancer Res. Pract.*, **4**, 127 (2017); https://doi.org/10.1016/j.jcrpr.2017.07.001
3. C.L. Sutton, C.D. McKinney, J.E. Jones and S.B. Gay, *Radiographics*, **12**, 853 (1992); https://doi.org/10.1148/radiographics.12.5.1529129
4. Z. Momenimovahed, A. Tiznobaik, S. Taheri and H. Salehiniya, *Int. J. Womens Health*, **11**, 287 (2019); https://doi.org/10.2147/IJWH.S197604
5. N.S. Murthy, S. Shalini, G. Suman, S. Pruthvish and A. Mathew, *Asian Pac. J. Cancer Prev.*, **10**, 1025 (2009).
6. F. Bray, J. Ferlay, I. Soerjomataram, R.L. Siegel, L.A. Torre and A. Jemal, *CA Cancer J. Clin.*, **68**, 394 (2018); https://doi.org/10.3322/caac.21492
7. R. Foster, R.J. Buckanovich and B.R. Rueda, *Cancer Lett.*, **338**, 147 (2013); https://doi.org/10.1016/j.canlet.2012.10.023
8. J. Swanner, J. Mims, D.L. Carroll, S.A. Akman, C.M. Furdui, S.V. Torti and R.N. Singh, *Int. J. Nanomedicine*, **10**, 3937 (2015); https://doi.org/10.2147/IJN.S80349
9. Q. Yue, G. Gao, G. Zou, H. Yu and X. Zheng, *BioMed Res. Int.*, **2017**, 8412508 (2017); https://doi.org/10.1155/2017/8412508
10. S.Y. Yin, W.C. Wei, F.Y. Jian and N.S. Yang, *Evid. Based Complement. Alternat. Med.*, **2013**, 302426 (2013); https://doi.org/10.1155/2013/302426
11. D.O. Kennedy and E.L. Wightman, *Adv. Nutr.*, **2**, 32 (2011); https://doi.org/10.3945/an.110.000117
12. D.W. Nyamai, W. Arika, P. Ogola, E. Njagi and M. Ngugi, *J. Pharmacogn. Phytochem.*, **4**, 2321 (2016).
13. Y. Qiansheng, Y. Jie, L. Huamin, C. Aocheng, C. Qinghua, W. Yongqi and H. Lan, *J. Beijing Normal Univ. Nat. Sci. Ed.*, **42**, 70 (2006).
14. L. He, J. Hou, M. Gan, J. Shi, S. Chantrapromma, H.K. Fun, I.D. Williams and H.H.-Y. Sung, *J. Nat. Prod.*, **71**, 1485 (2008); https://doi.org/10.1021/np800242w
15. V. Ahluwalia, R. Sisodia, S. Walia, O.P. Sati, J. Kumar and A. Kundu, *J. Pest Sci.*, **87**, 341 (2014); https://doi.org/10.1007/s10340-013-0542-6
16. C. Wang, R. Yang, L. Song, B. Ning, C. Ou-yang, A. Cao and L. He, *Phytochem. Lett.*, **16**, 245 (2016); https://doi.org/10.1016/j.phytol.2016.04.002
17. N. Ramya, P.K. Mayuri, A.S. Santny and T. Angayarkanni, *Asia Pacific J. Res.*, **1**, 170 (2015).
18. L. Samuel, Lalrotluanga, R.B. Muthukumaran, G. Gurusubramanian and N. Senthilkumar, *Exp. Parasitol.*, **141**, 112 (2014); https://doi.org/10.1016/j.exppara.2014.03.020
19. A.K. Chakravarty, T. Mazumder and S.N. Chatterjee, *Evid. Based Complement. Alternat. Med.*, **2011**, 471074 (2011); https://doi.org/10.1093/ecam/neq033
20. C.L. Ringmichon and B. Gopalkrishnan, *Int. J. Appl. Biol. Pharm. Technol.*, **8**, 1 (2017).
21. V. Ralte and S. Lallianrawna, *Sci. Vision*, **14**, 128 (2014).
22. S.K. Mandal, R. Boominathan, B. Parimaladevi, S. Dewanjee and S.C. Mandal, *Indian J. Exp. Biol.*, **43**, 662 (2005).
23. H. Chen, B. Zhou, J. Yang, X. Ma, S. Deng, Y. Huang, Y. Wen, J. Yuan and X. Yang, *Front. Pharmacol.*, **9**, 483 (2018); https://doi.org/10.3389/fphar.2018.00483
24. Y.-S. Li, H. Zou, N. Zhu, W. Li, X.-Y. Na, S.-Z. Tang and Y.Z. Yang, *J. Southwest Agric. Univ.*, **22**, 331 (2000).

25. Y. Jin, L. Hou, M. Zhang, Z. Tian, A. Cao and X. Xie, *Crop Prot.*, **60**, 28 (2014); https://doi.org/10.1016/j.cropro.2014.02.008
26. S. Mani, K. Natesan, K. Shivaji, M.G. Balasubramanian and P. Ponnusamy, *Biocatal. Agric. Biotechnol.*, **22**, 101381 (2019); https://doi.org/10.1016/j.bcab.2019.101381
27. S. Hemmati, A. Rashtiani, M.M. Zangeneh, P. Mohammadi, A. Zangeneh and H. Veisi, *Polyhedron*, **158**, 8 (2019); https://doi.org/10.1016/j.poly.2018.10.049
28. A.R. Jalalvand, M. Zhaleh, S. Goorani, M.M. Zangeneh, N. Seydi, A. Zangeneh and R. Moradi, *J. Photochem. Photobiol. B*, **192**, 103 (2019); https://doi.org/10.1016/j.jphotobiol.2019.01.017
29. M. Look, A. Bandyopadhyay, J.S. Blum and T.M. Fahmy, *Adv. Drug Deliv. Rev.*, **62**, 378 (2010); https://doi.org/10.1016/j.addr.2009.11.011
30. A. Zangeneh, M. Pooyanmehr, M.M. Zangeneh, R. Moradi, R. Rasad and N. Kazemi, *Comp. Clin. Pathol.*, **28**, 1507 (2019); https://doi.org/10.1007/s00580-019-03007-9
31. M.M. Zangeneh, A. Zangeneh, E. Pirabbasi, R. Moradi and M. Almasi, *Appl. Organomet. Chem.*, **33**, e5246 (2019); https://doi.org/10.1002/aoc.5246
32. S. Goorani, M.K. Koohi, H. Morovvati, J. Hassan, A. Ahmeda and M.M. Zangeneh, *Appl. Organomet. Chem.*, **34**, e5475 (2020); https://doi.org/10.1002/aoc.5475
33. S. Hemmati, Z. Joshani, A. Zangeneh and M.M. Zangeneh, *Appl. Organomet. Chem.*, **34**, e5277 (2020); https://doi.org/10.1002/aoc.5277
34. M.S. Akhtar, M.K. Swamy, A. Umar and A.A. Al Sahli, *J. Nanosci. Nanotechnol.*, **15**, 9818 (2015); https://doi.org/10.1166/jnn.2015.10966
35. G.R. Rudramurthy, M.K. Swamy, U.R. Sinniah and A. Ghasemzadeh, *Molecules*, **21**, 836 (2016); https://doi.org/10.3390/molecules21070836
36. A.K. Mittal, K. Thanki, S. Jain and U.C. Banerjee, *Appl. Nanomed.*, **1**, 1 (2016).
37. K. Elangovan, D. Elumalai, S. Anupriya, R. Shenbhagaraman, P.K. Kaleena and K. Murugesan, *J. Photochem. Photobiol. B*, **151**, 118 (2015); https://doi.org/10.1016/j.jphotobiol.2015.05.015
38. S. Gurunathan, J.W. Han, V. Eppakayala, M. Jeyaraj and J.H. Kim, *BioMed Res. Int.*, **2013**, 535796 (2013); https://doi.org/10.1155/2013/535796
39. S. Gurunathan, J.W. Han, J.H. Park, E. Kim, Y.J. Choi, D.N. Kwon and J.H. Kim, *Int. J. Nanomedicine*, **10**, 6257 (2015); https://doi.org/10.2147/IJN.S92449
40. S. Gurunathan, J.K. Jeong, J.W. Han, X.F. Zhang, J.H. Park and J.H. Kim, *Nanoscale Res. Lett.*, **10**, 35 (2015); https://doi.org/10.1186/s11671-015-0747-0
41. J.-C. Liou, C.-C. Diao, J.-J. Lin, Y.-L. Chen and C.-F. Yang, *Nanoscale Res. Lett.*, **9**, 1 (2014); https://doi.org/10.1186/1556-276X-9-1
42. S. Sahu, N. Sinha, S.K. Bhutia, M. Majhi and S. Mohapatra, *J. Mater. Chem. B Mater. Biol. Med.*, **2**, 3799 (2014); https://doi.org/10.1039/C3TB21669A
43. C.V. Jagannath and B.K. Radheshyam, *World J. Pharm. Pharm. Sci.*, 1574 (2017); https://doi.org/10.20959/wjpps20174-8945
44. S.K. Gautam, Y. Baid, P.T. Magar, T.R. Binadi and B. Regmi, *Int. J. Appl. Sci. Biotechnol.*, **9**, 128 (2021); https://doi.org/10.3126/ijasbt.v9i2.37822
45. T. Mosmann, *J. Immunol. Methods*, **65**, 55 (1983); https://doi.org/10.1016/0022-1759(83)90303-4
46. D. Srivastava, G. Joshi, K. Somasundaram and R. Mulherkar, *Anticancer Res.*, **31**, 3851 (2011).
47. C. Pereira, M.S. Santos and C. Oliveira, *Neurobiol. Dis.*, **6**, 209 (1999); https://doi.org/10.1006/nbdi.1999.0241
48. S.M. Bhosle, N.G. Huilgol and K.P. Mishra, *Clin. Chim. Acta*, **359**, 89 (2005); https://doi.org/10.1016/j.cccn.2005.03.037
49. D. Baskic, S. Popovic, P. Ristic and N.N. Arsenijevic, *Cell Biol. Int.*, **30**, 924 (2006); https://doi.org/10.1016/j.cellbi.2006.06.016
50. N.A. Franken, H.M. Rodermond, J. Stap, J. Haveman and C. Van Bree, *Nat. Protoc.*, **1**, 2315 (2006); https://doi.org/10.1038/nprot.2006.339
51. N. Ingarsal, V. Kasthuri and S. Ananth, *Ann. Rom. Soc. Cell Biol.*, **25**, 2988 (2021).
52. A.A. Akinsiku, E.O. Dare, K.O. Ajanaku, J.A. Adekoya and J.I. Ayo-Ajayi, *J. Mater. Environ. Sci.*, **3**, 902 (2018); https://doi.org/10.26872/jmes.2018.9.3.100
53. A. León, P. Reuquen, C. Garín, R. Segura, P. Vargas, P. Zapata and P.A. Orihuela, *Appl. Sci.*, **7**, 49 (2017); https://doi.org/10.3390/app7010049
54. Y. Meng, *Nanomaterials*, **5**, 1124 (2015); https://doi.org/10.3390/nano5021124
55. A. Hossain, Y. Abdallah, M.A. Ali, M.M.I. Masum, B. Li, G. Sun, Y. Meng, Y. Wang and Q. An, *Biomolecules*, **9**, 863 (2019); https://doi.org/10.3390/biom9120863
56. N. Babu, V.M. Pathak and A. Singh, *Pharma Innov.*, **8**, 817 (2019).
57. A. Gnanasoundari, S. Nagamani and P. Thangamathi, *Int. J. Lifesciencs*, **3**, 127 (2015).
58. S. Ananth and P. Thangamathi, *Int. J. Biol. Sci.*, **8**, 20 (2018).
59. S.J. Joshi, S.J. Geetha, S. Al-Mamari and A. Al-Azkawi, *Jundishapur J. Nat. Pharm. Prod.*, **13**, e67846 (2018); https://doi.org/10.5812/jjnpp.67846
60. Y.G. Yuan, Q.L. Peng and S. Gurunathan, *Int. J. Nanomedicine*, **12**, 6487 (2017); https://doi.org/10.2147/IJN.S135482
61. K. Khanra, S. Panja, I. Choudhuri, A. Chakraborty and N. Bhattacharyya, *Nano Biomed. Eng.*, **8**, 39 (2016); https://doi.org/10.5101/nbe.v8i1.p39-46
62. S.R. Palle, J. Penchalaneni, K. Lavudi, S.A. Gaddam, V.S. Kotakadi and V.N. Challagundala, *Lett. Appl. Nano Bio. Sci.*, **9**, 1165 (2020); https://doi.org/10.33263/LIANBS93.11651176
63. K. Cao, J. Yang, C. Lin, B.N. Wang, Y. Yang, J. Zhang, J. Dai, L. Li, C. Nie, Z. Yuan and M. Li, *Cancer Biother. Radiopharm.*, **27**, 259 (2012); https://doi.org/10.1089/cbr.2011.1126
64. S. Gurunathan, J.H. Park, J.W. Han and J.H. Kim, *Int. J. Nanomedicine*, **10**, 4203 (2015); https://doi.org/10.2147/IJN.S83953
65. Y.G. Yuan, S. Zhang, J.Y. Hwang and I.K. Kong, *Oxid. Med. Cell. Longev.*, **2018**, 6121328 (2018); https://doi.org/10.1155/2018/6121328
66. K. Khanra, S. Panja, I. Choudhuri, A. Chakraborty and N. Bhattacharyya, *Nanomed. J.*, **3**, 15 (2016).
67. M.A. Rathi, *Pharmacology*, **1**, 33 (2018).
68. J.D. Hayes, A.T. Dinkova-Kostova and K.D. Tew, *Cancer Cell*, **38**, 167 (2020); https://doi.org/10.1016/j.ccell.2020.06.001
69. C.R. Reczek and N.S. Chandel, *Annu. Rev. Cancer Biol.*, **1**, 79 (2017); https://doi.org/10.1146/annurev-cancerbio-041916-065808
70. J.W. Han, S. Gurunathan, Y.J. Choi and J.H. Kim, *Int. J. Nanomedicine*, **12**, 7529 (2017); https://doi.org/10.2147/IJN.S145147
71. J.W. Han, J.K. Jeong, S. Gurunathan, Y.J. Choi, J. Das, D.N. Kwon, S.-G. Cho, C. Park, H.G. Seo, J.-K. Park and J.-H. Kim, *Nanotoxicology*, **10**, 361 (2016); https://doi.org/10.3109/17435390.2015.1073396
72. C.D. Fahrenholtz, J. Swanner, M. Ramirez-Perez and R.N. Singh, *J. Nanomater.*, **2017**, 5107485 (2017); https://doi.org/10.1155/2017/5107485
73. D.C. Chan, *Ann. Rev. Pathol.: Mechanisms of disease*, **15**, 235 (2020); https://doi.org/10.1146/annurev-pathmechdis-012419-032711.
74. B.C. Dickinson and C.J. Chang, *Nat. Chem. Biol.*, **7**, 504 (2011); https://doi.org/10.1038/nchembio.607
75. H.J. Ahn, K.I. Kim, G. Kim, E. Moon, S.S. Yang and J.S. Lee, *PLoS One*, **6**, 28154 (2011); https://doi.org/10.1371/journal.pone.0028154
76. T.S. Kamatchi, M.K. Mohamed Subarkhan, R. Ramesh, H. Wang and J.G. Malecki, *Dalton Trans.*, **49**, 11385 (2020); https://doi.org/10.1039/D0DT01476A
77. Y.-J. Choi, J.-H. Park, J. Han, E. Kim, O. Jae-Wook, S. Lee, J.-H. Kim and S. Gurunathan, *Int. J. Mol. Sci.*, **17**, 2077 (2016); https://doi.org/10.3390/ijms17122077